ENHANCEMENT OF PA-TFC RO MEMBRANE BY USING INORGANIC NANOPARTICLES

Yehia A. Shebl[1], Yousra H. Kotp[2], Hosam A. Shawky[2] Mohamed S. El-Deab[1], Bahgat E. El-Anadouli[1],

[1]Chemistry Department, Faculty of Science, Cairo University, P.O.B 12613 -Giza, Egypt.
[2]Egyptian Desalination Research Center of Excellence (EDRC), Desert Research Center, Cairo, P.O.B 11753, Egypt,E-mail address: yosra.kotp@edrc.gov.eg

ABSTRACT

This study focuses on to the change of the execution of polyamide (PA) thin-film composite (TFC) reverse osmosis (RO) membrane utilizing surface alteration by $MgSiO_3$ nanoparticles. This has been an expert by means of holding of the practical grafting of PA layer with magnesium silicate nanoparticles ($MgSiO_3$) in the presence of 2-acylamido 2-methyl propane sulphonic acid (AMPS) as condensing monomer. To confirm the presence of $MgSiO_3$ nanoparticles and to inspect the morphology of the TFC nanoparticles layer SEM, FT-IR, XRD, analysis were used. The contact angel estimations demonstrate an increase in the hydrophilicity of the thin film surface by the addition of nanoparticles. The water flux and salt rejection of the modified membranes were 25 L/m^2h and 95.5%, respectively.

Keywords: Membrane performance, Reverse osmosis, Water desalination, Thin film composite, Magnesium silicate nanoparticle

1 INTRODUCTION

Egypt, has entered a state where its national economic development is under a significant negative stress as the deficiency of the available freshwater sources. Egypt has already reached a sign of scarcity where the threshold rate is about (1000m3/capita/year) in the nineties. As a limit of absolute shortage (500m3/ca/yr) is utilized, this will be clear with populace forecast for 2025 which will take Egypt down to 500m3/ca/yr [1].

Water desalination has the ability to get freshwater from various kinds of water sources that without desalination not to be fit for different human uses. Water desalination has a several proven and fixed technologies which supply the water for the population in regions those have insufficient fresh water sources or to furnish ultrapure water for the industrial process. Currently, it is assessed that there are more than 18000 desalination plants in the service in more than 150 nations around the globe produce a total capacity up to 86.5 million cubic meters per day; a great portion of them in the Middle East and the quantity is continuously growing. Membrane technology shared about 70% of the total capacity of global desalted water and about 65% of them are RO membrane separation plants while about only 28% are thermal desalination plants [2]. Commercial interest in Reverse Osmosis technology and the rate of installed RO desalination stations has been expanding steadily over the recent 10 years due to continuous process improvements, mainly the striking advances in the membrane properties, the great development of the energy recovery devices efficiency, also improvements in the module layout, process design, and feed pretreatment resulting in the huge decline in overall water production costs [3].

Uses of nanotechnology could offer remarkable development and improvement to water treatment process, also offer significant solutions for current and future freshwater demands, additionally, provide favorable solutions for water quality challenges. Incorporation of a functional nanomaterial inside the

layers of the polymer membrane for the manufacture of which was agreed to be called Mixed Matrix membrane that consisting of an inorganic filler (with excellent thermal, biological and chemical stabilities) like zeolite, metal oxide, carbon nanotubes, silver and silica nanoparticles dispersed in the continuous thin polymeric phase (with high performance flexibility and processability properties) through the interfacial polymerization process, has been Used widely to offers a great possibility to enhance permeability, fouling resistance, also mechanical and thermal stability of the desalination membrane [4].

One of the key parameters for the effective execution of nanocomposite MMMs is to enhance the scattering of inorganic nanomaterial fillers in polymer lattice through the foundation of particular and strong synergy between the nanofiller and the polymer matrix [5]. Perversely, the weak interfacial adaptability of the dispersed nanofiller through the polymer leads to nanofiller agglomeration, which gives rise to the development of unintended voids in the membranes, and therefore nanofiller may be leached especially after a period of operation and susceptible to long term of the required operating pressure and also the cleaning process of the membrane. This eventually leads to hindered membrane properties and its lifetime, add to that health risks and environmental hazards of the discharged nonmaterial [6]. So here in this study, we development of a MMM by making a surface modification via attachment of inorganic nanoparticles like magnesium silicate nanoparticles (MgSiO3NPs) as a coating layer covering a routine TFC membrane to couple the two different properties of organic and inorganic substances like high processability of and high activity of organic polymers, as far as brilliant thermal and chemical stabilities, high selectivity and high permeability, of inorganic materials.The chemical structure and the morphology of the membrane grafted and modified with nanoparticles were studied and characterized by X-ray diffraction (X-ray), infrared spectroscopy (FTIR), Scanning electron microscope (SEM), and contact angle (CA) determination. Optimization of the amount of $MgSiO_3$NPs incorporated onto the TFC surface was proposed leading to the best RO membrane performance.

2 EXPERIMENTAL

2.1. Materials

Polysulfone pellets Udel P-3500 were provided by Solvay advanced polymer, USA, N,N-dimethylacetamide (DMA) were supplied from (Sigma-Aldrich). metaphenylenediamine (MPDA), trimesoyl chloride (TMC), triethyl amine (TEA), (+)-10-champhor sulfonic acid (CSA), sodium lauryl sulfate (SLS), 2-acrylamido-2-methyl propane sulfonic acid (AMPS), potassium persulfate $\geq$ 99.0%, sodium metabisulfite $\geq$ 99.0%, and a commercial form of nano-magnesium silicate ($MgSiO_3$) (diameter of particles about 15 nm) was afforded from Dixiang Chemical Engineering Co., Ltd. (Shanghai, China). Other reagents such as n-hexane, sodium chloride (NaCl) are of analytical grade.

2.2. Characterization of $MgSiO_3$ NPs.

Scanning electron microscope (*SEM Model Quanta FEG*) connected with EDX Unit, with speeding up voltage 30 K.V., magnification 250x up to 20000x and resolution for gun 1m also XRD analysis utilizing (*Shimadzu X-ray*) diffractometer, (*Model XD 490 Shimadzu, Kyoto, Japan)* and FTR-IR analysis (*Nicolet avator 230 spectrometer*) at room temperature were used to characterize the morphology of $MgSiO_3$ NPs.

2.3. Preparation of microporous polysulfone support membrane

PS casting solution was prepared by melting 15 wt. % PSF in DMA at 80–90 ◦C with continuous stirring. The resultant polysulfone solution was molding onto a glass tray and coagulates in a water bath. After 10 min of gelation, the resulting PSF membrane was washed with bidistilled water to remove the

residual DMA. The prepared PSF support membrane was saved in distilled water for at minimal 24 hr before use.

2.4. Manufacture of thin film composite membranes

Aromatic polyamide TFC RO membranes were synthesized by the interfacial polymerization of MPD (2.0 wt. %) in aqueous phase and Trimethoyl chloride (0.15 wt. %) in organic phase (n-hexane), CSA (4.0 wt. %), SLS (0.15 wt. %), and TEA (3 wt. %), were combined into the aqueous phase. CSA and SLS were used to improve the absorption of MPD in microporous polysulfone support membrane. TEA hurried the MPD–TMC reaction by eliminating hydrogen halide created during amide bond formation [7]. Firstly, the support membrane was soaked with MPD solution for two minutes. The overabundance solution was removed by a rubber roller. Then the support membrane covered with 0.15 wt % of TMC-hexane solution for the 60s, followed by rinsing with n-hexane and cured at 80 ◦C for 10min. This resulted in the creation of ultra-thin aromatic polyamide film over the support membrane that was denoted as "parent membrane" in this work. The membranes then washed and preserved in deionized water before characterization tests or application studies.

2.5. Fabrication of $MgSiO_3$ NPs modified AMPS-g-TFC membranes

Firstly redox grafting was performed utilizing a blend of redox initiators consisting of potassium persulfate $K_2S_2O_8$ (2% of monomers) and sodium metabisulfite $Na_2S_2O_5$ (1/3 of $K_2S_2O_8$) on a newly fabricated TFC flat sheet membrane for about 20 minutes. Secondly a different mixture of various concentrations of (AMPS) monomer (2.5-15%) and ($MgSiO_3$) nano-particles (0.005-0.1% of monomer concentration) were sonicated for one hour, then added to the above initiated TFC flat sheet membrane, and immediately put in the oven to complete the reaction at varied temperatures and different times (Scheme 1).

2.6. Membrane characterization

The thin film composite RO membrane surface was characterized by Fourier transform infrared (FT-IR) made with a (*Nicolet avator 230 spectrometer*) at room temperature. Irtran crystal at a 45° angle of downfall employed for FT-IR analysis of different samples. Scanning electron microscopy (SEM) with (*SEM Model Quanta FEG*) connected with EDX Unit, with speeding up voltage 30 K.V., magnification 250x up to 20000x and resolution for gun 1m was used for examination of membrane morphology. Samples are coated with gold. X-ray diffraction patterns were performed utilizing (*Shimadzu X-ray*) diffractometer, (*Model XD 490 Shimadzu, Kyoto, Japan)* with a nickel filter and Cu-K_α radiation tube. Also, the surface hydrophilicity of the films was estimated by a contact point goniometer from (VCA Video Contact Angle System, Kr ÜssDSA25B, Germany) at room temperature.

2.7. Performance test

ALFA LAVAL pilot-scale laboratory unit for membrane filtration (*Model LabUnit M20*) was used for testing the performance of synthesized reverse osmosis membranes (Fig. 1). Flat sheet layers with a viable region of 0.018 m^2 were set in the test instrument with the polyamide dynamic layer confronting the bolster water. All film tests were carried and tried at minimum twice with a sum of three layers tests for RO execution, the normal outcomes were taken, the volume of penetrating was taken in 1 hr and the flux communicated regarding (L/m^2h).

3 RESULTS AND DISCUSSION

3.1. $MgSiO_3$ NPs characteristics

It was clear from SEM image in Fig.2, $MgSiO_3$ NPs are well distributed, of spherical morphology and of very small and highly agglomerated particles with a rounded shape.The functional groups of the $MgSiO_3$ NPs were resolved using the FTIR spectrum as presented in Fig.3. A peak at 3697 cm^{-1} is characteristic to Mg–OH stretching, broadening peak near 3437 cm^{-1} attributable to H-bonding of coordinated water and the strong peak at 1017 with a shoulder band at 878 cm^{-1} is due to the existence of Si–O stretching vibrations, while the Mg–O vibrations occur at 462 cm^{-1} [8]. X-ray diffraction displays crystalline structures (Fig. 4), where, three minor peaks demonstrate that the materials have identical patterns of crystalline nature.Also, the three minor peaks evidenced at 18–38, 51 and 58–62 °2θ were pointed out to $MgSiO_3$ NPs.

3.2. Spectroscopic characterizations of PSF, TFC, AMPS-g-TFC and $MgSiO_3$ NPs modified AMPS-g-TFC membranes.

FTIR was performed to describe the successful preparation of the $MgSiO_3$ NPs modified AMPS-g-TFC membrane. Figure 5, shows the characteristic peaks of PSF support layer and shows bands at737.1, 851.9, 1013, 1151.78, 1484 and 1579 cm^{-1} corresponding to (aromatic hydrogen), isolated aromatic hydrogen, ether group, sulfonic group, alkane groups and C-H aromatics respectively [9,10]. While in the TFC membrane Fig.5 elucidate different new peak bands appeared indicating the coating of PA barrier layer onto the PSF support layer. Two peak bands appear around 1597 cm^{-1} and 1248 cm^{-1} for the C=O stretching vibration and C-N group of the amide II on TFC membrane, respectively [11].The spectrum reveals that there is a strong band around 1675.8cm^{-1}, which is characteristic of C=O band of an amide group (amide I). Also, a small peak at 1777.09 cm^{-1} which corresponded to C=O stretching (acid). The stretching peak at 3341 to 3473cm^{-1} can be assigned to N-H and O-H which overlapped together [12,13]. The FTIR spectra of the AMPS-g-TFC membranes appeared in Fig.5, where also the NH2 and C=O bands for TFC membrane, we observe specific absorption peak of AMPS monomer at 1294 cm-1 because of the S-O group in the sulfonic acid (SO2) asymmetric and at 1152 cm-1 due to symmetric bands of (S-O) both referred by [13], who state 1250–1150 and 1100–1000 cm-1, respectively. The stretching band of OH group for sulfonic acid resemble at 3000 cm-1. As showed in Scheme (1), the specific absorption peak at (~1654cm-1) resulted from the stretching vibration of C=O of the amide (-CONH2) group, this descending in the frequency peak of the carbonyl group because of the hydrogen bonds developed with N-H groups at the probable grafting position on the surface of TFC membrane [14]. Also, the distinct peak at 1081 cm-1 is an outcome of the behavior of S=O stretching in –SO3 of AMPS. Additionally, The peaks exhibit at the range from ~2970 and ~3064 cm–1 resembles C–H stretching vibrations of –CH3 and –CH2, of AMPS [15].

By examine the MgSiO3 NPs modified AMPS-g-TFC membrane spectrum and match it with the primary TFC membrane as presented in the Fig.5, it illustrated the existing of the new specific stretching band with 1904 cm-1 as a result of Si-O stretching vibrations for MgSiO3 NPs [16]. The spectra also showed a wide band around 3600 cm-1 which represent an intermolecular hydrogen bond established by the covalent connection of the carbonyl Oxygen of AMPS to the hydroxyl group associated with MgSiO3 NPs [17], as the appearing of The peak at about 3900 cm -1 is may be attributed to silica-water interaction of Si-OH vibration style [18]. So as a result of adding MgSiO3NPs to the AMPS grafting solution leading to shifting the C=O stretching vibrational peak due to delocalization of electrons distribution across the unsaturated system which stabilizes it by lowering its energy in the presence of electron donated from the Mg atoms this aspect agrees with the hypothesis revealed in the literature [19]. conclusively, these peaks

suggest the succeeded combination of MgSiO3 NPs with AMPS grafting monomer as a surface coating of TFC membrane.

Investigation of surface nature of TFC membrane were investigated by X-ray diffraction (XRD) technique .In Fig.6, the typical diffraction peak for pure PSF is recognized at a 2θ value of 18.00. The spectrum exhibited the highly amorphous character of PSF [20]. The broad peak at 18.00 (2θ) resembled with low crystallinity, while the x-ray diffraction peak of TFC membrane appears at a 2θ value of 18.01. Also, the presence of wide curves with moderate intensity centered on 18 of 2θ of TFC, which indicate the presence of semicrystalline nature concerning to the composite membrane [21]. In addition to The crystalline part in the TFC is a result to the polyamide surface layer and the amorphous zone are due to PSF support layer. The broad peak center on every X-ray formula was referred to the average intersegmental distance of polymer main chains [22]. Fig.6, reports the XRD pattern of AMPS-g-TFC membranes which are crystalline in nature and give three crystalline peaks at 2θ angles of 26.2, 38,1 and 44.4 with the union of the dispersal peak concerning amorphous PS, nevertheless mean that their position is moderately shifted [23]. The MgSiO3NPs modified AMPS g TFC membrane displays six crystalline specific peaks at angles 2, beside that the main fundamental peaks of MgSiO3 NPs with values of 2 equal 10 2 17 80 18 31 38 1 44 4 and 54 6. The XRD pattern explains that MgSiO3 NPs successfully integrated in the grafted layer above the pristine membrane surface. Table 1 detect the comparison in terms of peak position relative intensity FWHM and d space in the AMPS g TFC and MgSiO3NPs modified AMPS g TFC membranes.

3.3. Microscopic characterizations of the PSF support layer, PSF/TFC, and TFNC membrane.

As the surface morphology have a significant contribution to the resulted membrane performance The surface layer structures of PSF TFC AMPS g TFC and MgSiO3NPs modified AMPS g TFC membranes were distinguished by SEM as displayed in Fig 7 Figure 7 a presents the PSF layer is highly porous with such as a finger like macro voids spongy–structure which can sustain high pressure [24]. Also from Figure 7 b we can observe very thin surface layer is rough and dense with a well formed “ridge and valley” asymmetric structure which is representative for a typical PA membrane [25]. Figure 7 c shows that the attachment of the grafted monomer was accompanied by an expansion in surface roughness and nodular morphology related to unchanged one. From SEM image in Fig 7 d we can observe the presence of MgSiO3NPs nanoparticles within the grafted layer which leads to more advancing in membrane surfaces roughness morphology also increasing not only in pore density but also in the size. We can suppose that the incorporation of MgSiO3NPs enhance the features of the membrane surface and create new stream channels through the thin layer making a direct impact on membrane water permeability Additionally the cross sectional SEM images of AMPS g TFC and MgSiO3 NPs modified AMPS g TFC membranes appeared in Fig. 8 a b which show that the surface modification achieved by this study results in a small increase in the thickness of the resulted membrane correlated to initial TFC membrane.

3.4. Hydrophilicity of the membranes

Figure10. Demonstrates the contact angle (θ) estimations of PSF, TFC, AMPS-g-TFC and MgSiO3 NPs modified AMPS-g-TFC membranes. From the Fig. 9 PSF substrate demonstrates contact angle equals to 72.8° this indicates week membrane surface wettability with water and moderately hydrophobic properties. After interfacial polymerization, the hydrophilicity of TFC membrane was enhanced, and it diminished to 68.3° this demonstrated the PA layer was reasonably hydrophilic, with modification of the TFC membrane by monomer AMPS grafting, the contact angle achieved 62.1°. The low contact angle of the AMPS-g-TFC layer demonstrated more hydrophilic properties indicated more hydrophilic properties because of the gatherings of polar and hydrophilic groups of sulfonic acids in the AMPS monomer

structure. Moreover, MgSiO3 NPs modified AMPS-g-TFC membrane exhibits the lowest contact angle which reached approximately 45.9° at 25˚C; confirm the excellent surface hydrophilicity owing to the still subsistence of free silicate species on membrane surfaces. Those free silicate groups act as a dynamic hydrophilic functional group on the membrane surface, that causes higher association in water and surface, through the favorable Si-OH forming groups. The considerable enlargement in membrane hydrophilicity produces increasing in the modified membrane permeability.

3.7. Performance evaluation

Membrane performance enhancement for desalination by surface coating with magnesium silicate nanoparticles using the free radical grafting technique. In this study, various parameters were studied such as the concentration of AMPS monomer, the concentration of $MgSiO_3$ NPs, grafting time and temperature to get the optimum condition necessary to prepare the best suitable $MgSiO_3$ NPs modified AMPS-g-TFC membrane for desalination of water which compared with pristine PA -TFC membrane.

3.7.1. Concentration of monomer AMPS and $MgSiO_3$ NPs.

Figures (10&11), show permeate water flux and the salt rejection of prepared membranes with various concentrations of AMPS monomer,& $MgSiO_3$ NPs respectively. It is observed that both permeate water flux and salt rejection increases with nanomaterial concentration increasing. Then, for higher concentrations, it decreases, this results can be clarified as the increasing of coating layers on the membrane could reduce the permeation flux. Also, the reduction in the salt rejection may be due to some coating layers could minimize the surface charge due to the concealment, which then minimizes the salt rejection due to the Donnan effect phenomena [26]. The results reflect the existence of an optimum concentration of AMPS monomer& $MgSiO_3$ NPs.

3.7.2. Grafting time and temperature.

By over increasing in grafting time or curing temperature as in Fig. (12&13), membranes water flux, and salt rejection have been decreased, this may be due to The decreasing of interchain hydrogen bonds as large amount of AMPS molecules were incorporated into aromatic polyamide chains, which may increase the polymer chain mobility, causing conformational alteration of aromatic polyamide chains. It might also create local destruction or compaction in the modified membrane surface and finally consequence in increased passing of both water and salt [27].

4 CONCLUSIONS

MgSiO3 NPs were attached to the surface of TFC membrane with AMPS monomer as a bridging agent via free radical grafting technique. MgSiO3 NPs modified AMPS-g-TFC membrane showed superior hydrophilic surface, as the contact angle with water reached (~45.9°). Microscopic and morphology of modified nanocomposite membrane also examined using FT-IR, XRD, and SEM. Furthermore, water flux and a salt rejection for the resulted membranes were assessed, where performance of the new modified membrane gave about 28.2 L/m2•h as a permeate water flux and a salt rejection of ≥95.5% was obtained for a saline water (2000 ppm of NaCl) at an applied pressure about 15 bars with a 32% increase in water flux comparing to the pristine TFC membrane. This study demonstrates that the MgSiO3 NPs modified AMPS-g-TFC membrane could remarkably enhance selectivity, water permeability and surface hydrophilic characters of membranes. These promising features of the modified membrane are possible to have a great impact on desalination process economics in terms of the capital and running costs.

ACKNOWLEDGMENTS

It is a pleasure to acknowledge the financial support provided by the Science and Technological Development Fund (STDF) in Egypt through Grant 5240 (Egyptian Desalination Research Center of Excellence, EDRC)

REFERENCES

Azmeera, Venkanna, P. Adhikary, and S. Krishnamoorthi. "Synthesis and characterization of graft copolymer of dextran and 2-acrylamido-2-methylpropane sulphonic acid." International Journal of Carbohydrate Chemistry 2012 (2012).

Arsuaga, María J. "Influence of the type, size, and distribution of metal oxide particles on the properties of nanocomposite ultrafiltration membranes." Journal of membrane science 2013; 428: 131-141.

Ali I M, Kotp Y H, El-Naggar I M. Thermal stability, structural modifications and ion exchange properties of magnesium silicate. Desalination. 2010; 259(1): 228-234.

Cassimatis, D., J. P. Bonnin, and T. Theophanides. "Donor–acceptor interactions in Friedel–Crafts systems. The CH3COCl• AlCl3 addition compound." Canadian Journal of Chemistry 48.24 (1970): 3860-3871.

de Aragão, Bernardo JG, and Younes Messaddeq. "Peak separation by derivative spectroscopy applied to FTIR analysis of hydrolized silica." Journal of the Brazilian chemical Society 19.8 (2008): 158
2-1594.
Dechant R, Danz W, Kimmer R, Schmolke Ultrarotspektroskopischeuntersuchungen an polymeren. (1972).

Deng, Baolin. "Effects of Polysulfone (PSf) Support Layer on the Performance of Thin-Film Composite (TFC) Membranes." J Chem Proc Eng 1 (2014): 1-8.

Kim, Ho S, Kwak S, Suzuki T. "Positron annihilation spectroscopic evidence to demonstrate the flux-enhancement mechanism in morphology-controlled thin-film-composite (TFC) membrane." Environmental science & technology 2005; 39(6): 1764-1770.

Kango, Sarita. Surface modification of inorganic nanoparticles for development of organic–inorganic nanocomposites—a review." Progress in Polymer Science. 2013; 38(8) 1232-1261.

Kang Y S, Lee S, Kim Y U, Shim S J. Kang YS, Lee SW, Kim UY, Shim YS. Pervaporation of water–ethanol mixtures through crosslinked and surface-modified poly (vinyl alcohol) membrane. J Memb Sci. 1990; 51: 215-226.

Kwak, Seung-Yeop, et al. "Correlations of chemical structure, atomic force microscopy (AFM) morphology, and reverse osmosis (RO) characteristics in aromatic polyester high-flux RO membranes." Journal of membrane science 132.2 (1997): 183-191.

Kwon, Young N, Tang C Y, Leckie J O. Change of membrane performance due to chlorination of crosslinked polyamide membranes. Journal of applied polymer science. 2006; 102(6): 5895-5902.

Lee, Soo H. Polyamide thin-film nanofiltration membranes containing TiO_2 nanoparticles. Desalination. 2008; 219(1): 48-56.

Li, Lei. Polyamide thin film composite membranes prepared from 3, 4′, 5-biphenyl triacyl chloride, 3, 3′, 5, 5′-biphenyl tetraacyl chloride and m-phenylenediamine. Journal of Membrane Science. 2007; 289(1): 258-267.

Lee, Peng K, Tom C A, Mattia D. A review of reverse osmosis membrane materials for desalination—development to date and future potential. Journal of Membrane Science. 2011; 370 (1): 1-22.

Ministry of Water Resources and Irrigation, Water Scarcity in Egypt, February 2014.

GWI (Global Water Intelligence) (2015). Section 1: Market profile. In: IDA Desalination Yearbook 2015-2016.

Noble, Richard D. "Perspectives on mixed matrix membranes." *Journal of membrane science* 378.1 (2011): 393-397.

Padmavathi, Rajangam, Karthikumar R, Sangeetha D. Multilayered sulphonated polysulfone/silica composite membranes for fuel cell applications. Electrochimica Acta. 2012; (71): 283-293.

Rao C N R. Chemical applications of infrared spectroscopy; Academic Press: New York, 1963.

Riccardi C S. Preparation of CeO_2 by a simple microwave–hydrothermal method. Solid State Ionics. 2009; 180 (2): 288-291.

Socrates, G. "Infrared Characteristic Frequencies, 2nd-Ed." (1994).

Sridhar S, Smitha B, Aminabhavi T M. Separation of carbon dioxide from natural gas mixtures through polymeric membranes - a review. Separation& Purification Reviews. 2007; 36(2): 113-174.

Song, Hui, Shu-Fen Zhang, Xi-Chen Ma, Da-Zhi Wang, and Jin-Zong Yang. "Synthesis and application of starch-graft-poly (AM-co-AMPS) by using a complex initiation system of CS-APS." Carbohydrate Polymers 69, no. 1 (2007): 189-195.

Tran, Ngon T., Taewoo Min, and Annaliese K. Franz. "Silanediol hydrogen bonding activation of carbonyl compounds." Chemistry–A European Journal 17.36 (2011): 9897-9900.

Xu, Guo-Rong, Wang J, Li C. Strategies for improving the performance of the polyamide thin film composite (PA-TFC) reverse osmosis (RO) membranes: surface modifications and nanoparticles incorporations. Desalination 2013; (328) : 83-100.

Wei, Xinyu. Surface modification of commercial aromatic polyamide reverse osmosis membranes by graft polymerization of 3-allyl-5, 5-dimethylhydantoin. Journal of Membrane Science. 2010; 351(1): 222-233.

Figure caption

Figure 1. Schematic diagram for LabUnit M 20 pilot-scale membrane filtration.

Figure 2. SEM images of magnesium silicate nanoparticles.

Figure 3. ATR-FTIR spectra magnesium silicate nanoparticles.

Figure 4. XRD images of magnesium silicate nanoparticles.

Figure 5. ATR-FTIR spectra of polysulfone (PSF) support layer, thin film composite membrane (TFC), AMPS-g-TFC membrane, and $MgSiO_3$NPs modified AMMPS-g-TFC membrane.

Figure 6. XRD images of polysulfone (PSF) support layer, thin film composite membrane (TFC), AMPS-g-TFC membrane, and $MgSiO_3$ NPs modified AMMPS-g-TFC membrane.

Figure 7. SEM images of top surface: (a) polysulfone support and (b) thin film composite membrane(TFC), (c) AMPS-g-TFC membrane, and (d) $MgSiO_3$ NPs modified AMMPS-g-TFC membrane.

Figure 8. Cross-section SEM images of: (a) AMPS-g-TFC membrane and (b) $MgSiO_3$ NPs modified AMMPS-g-TFC membrane.

Figure 9. Contact angles results of the surface of PSF support, thin film composite membrane, AMPS-g-TFC membrane, and $MgSiO_3$ NPs modified AMMPS-g-TFC membrane.

Figure 10. Effect of grafted AMPS monomer concentration on salt rejection and water flux of the resulting AMPS-g-TFC membrane testing with 2000 mg/l NaCl aqueous solution at 15 bar, 25°C (after 60 min.).
Figure 11. Effect of $MgSiO_3$ NPs concentration on salt rejection and water flux of the resulting $MgSiO_3$ NPs modified AMPS-g-TFC membrane testing with 2000 mg/l NaCl aqueous solution at 15 bar, 25°C (after 60 min.).

Figure 12. Effect of grafting temperature on salt rejection and water flux of the resulting $MgSiO_3$ NPs modified AMPS-g-TFC membrane testing with 2000 mg/l NaCl aqueous solution at 15 bar, 25°C (after 60 min.).

Figure 13. Effect of grafting time on salt rejection and water flux of the resulting $MgSiO_3$ NPs modified AMPS-g-TFC membrane testing with 2000 mg/l NaCl aqueous solution at 15 bar, 25°C (after 60 min.).

Scheme 1. Schematic diagram of grafting $MgSiO_3$ NP-AMPS modified monomer onto the surface of PA TFC membrane.

Scheme 2. Four expected mechanisms of the reaction and bonds formed between $MgSiO_3$ NPs and AMPS monomer to give $MgSiO_3$ NP-AMPS modified monomer which has been grafted on PA TFC membrane surface by free radical grafting technique.

Table caption
Table (1): XRD data of AMPS-g-TFC and MgSiO3 NPs Modified AMPS-g-TFC membranes.

Figure 1.

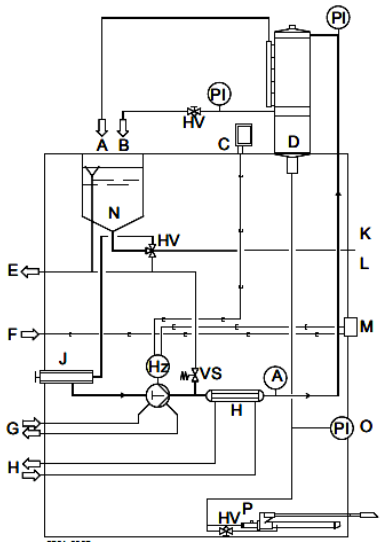

A = Permeate
B = Retentate
C = Cross-Flow Pump Control
D = Module
E = Drain/overflow
F = Electric Power (5m cable incl.)
G = Flushing water
H = Cooling/Heating water
J = Filter
K = To pump
L = To drain
M = Main switch
N = Tank 9 L.
O = Hydraulic oil pressure
P = Hydraulic oil pump

Figure2.

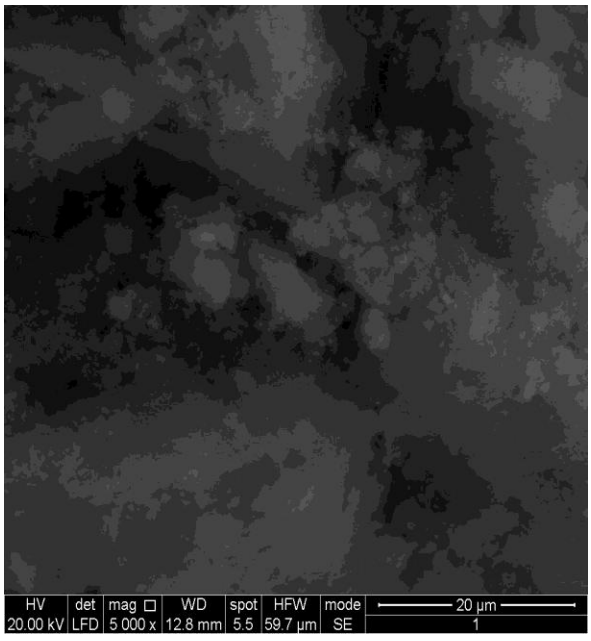

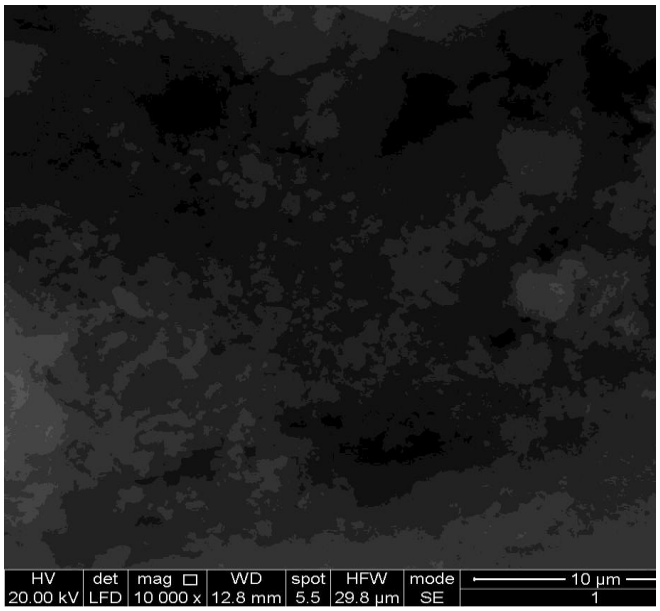

Figure3.

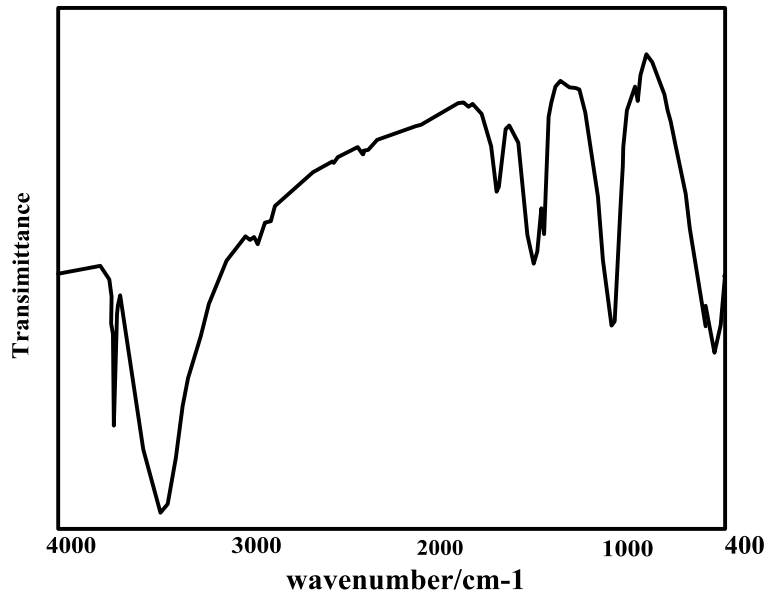

Figure4.

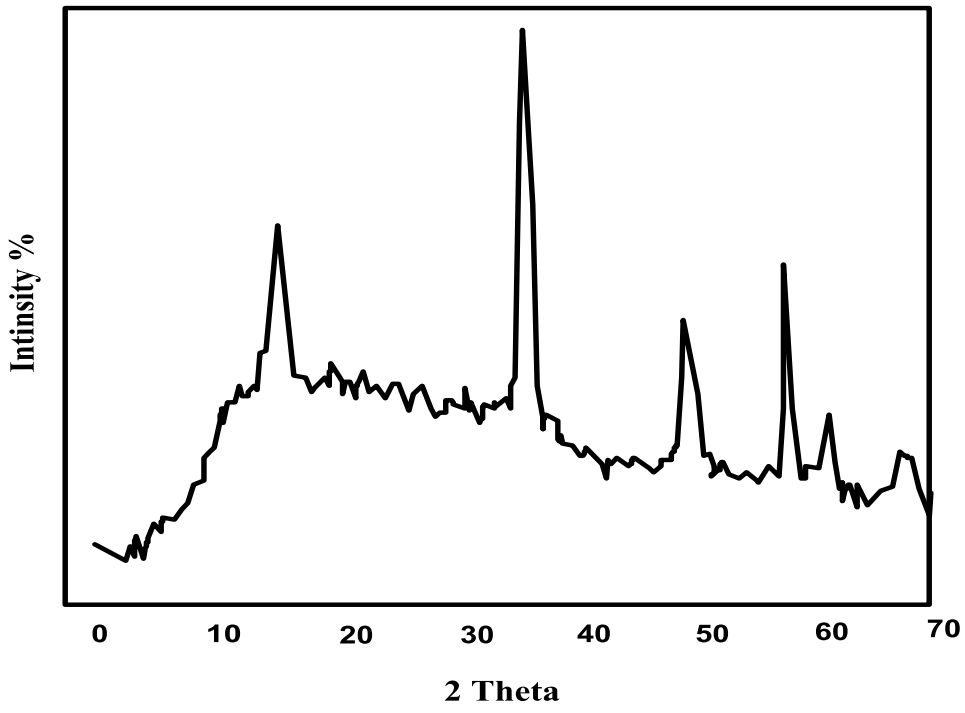

Figure 5.

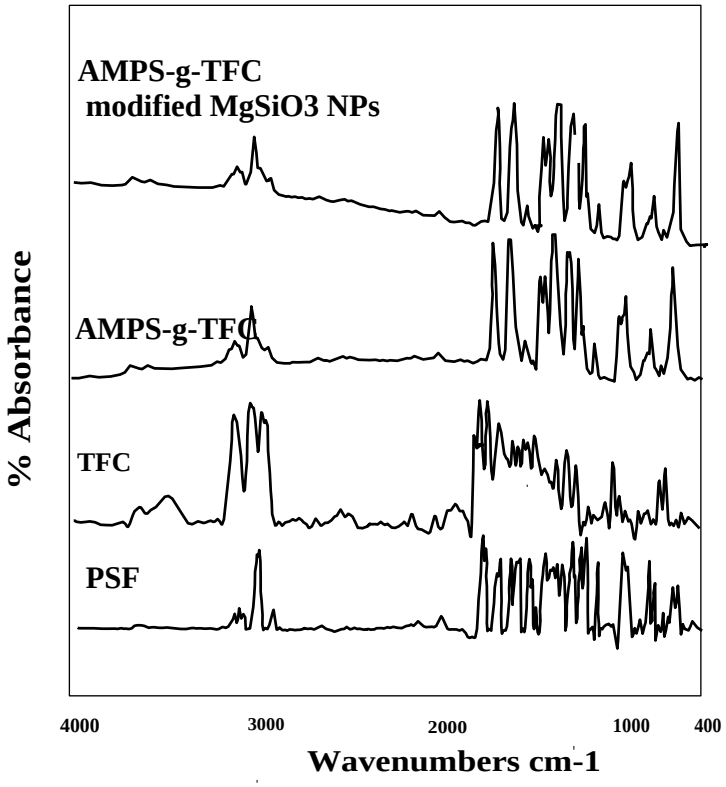

Figure 6.

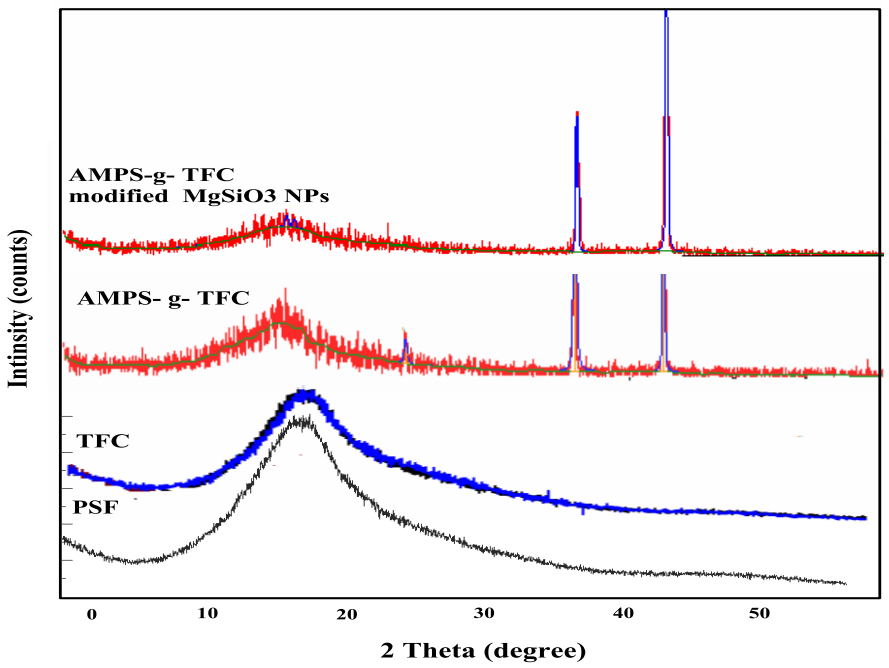

Figure7.

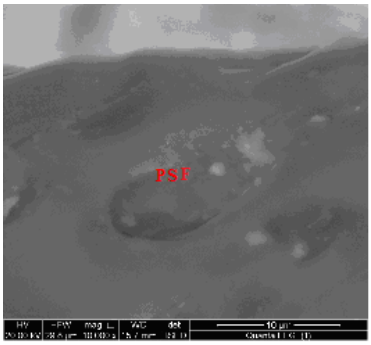

(a)

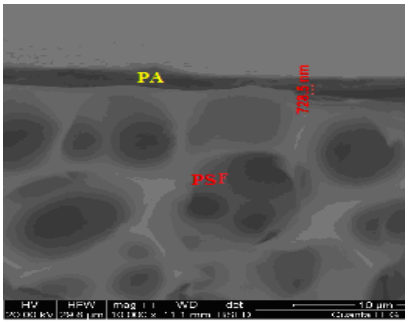

(b)

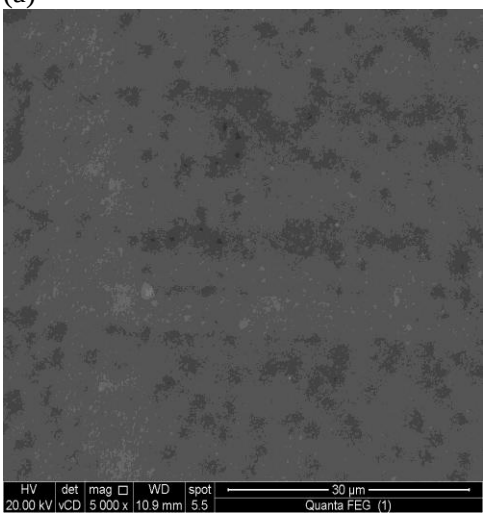

(c)

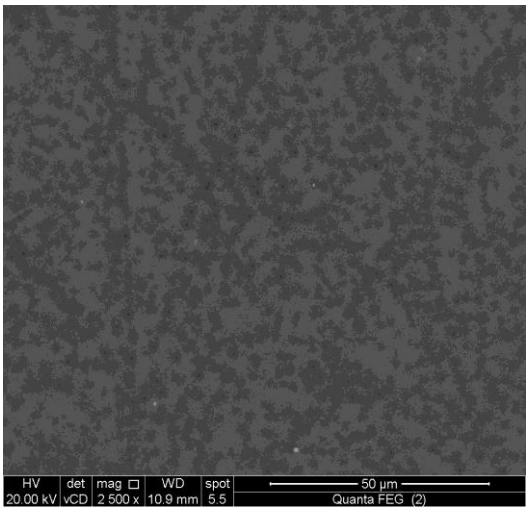

(d)

Figure8.

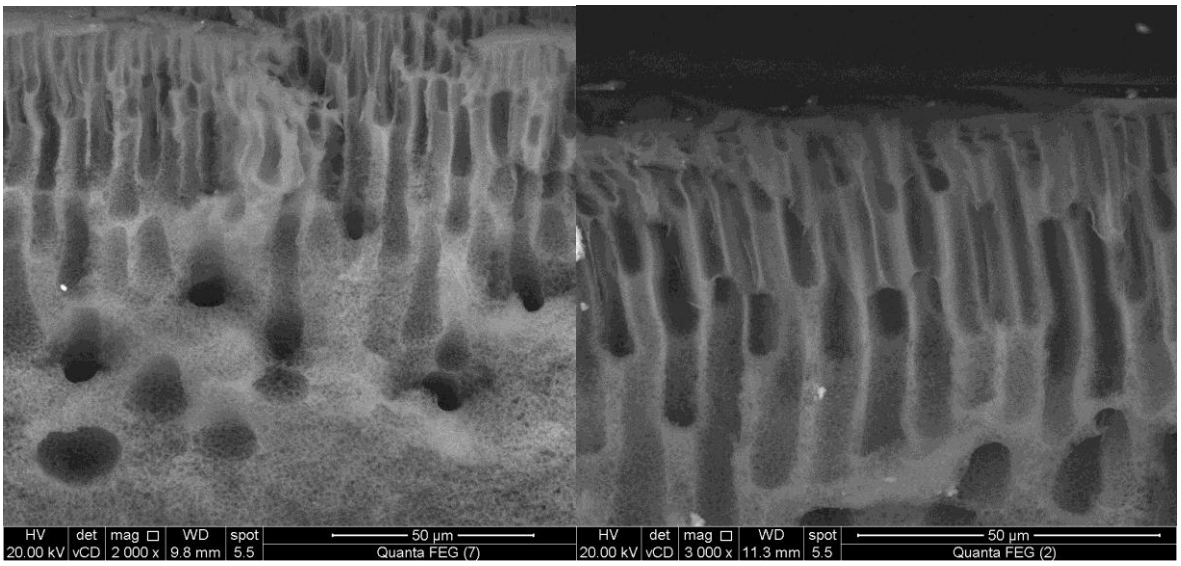

(a) **(b)**

Figure 9.

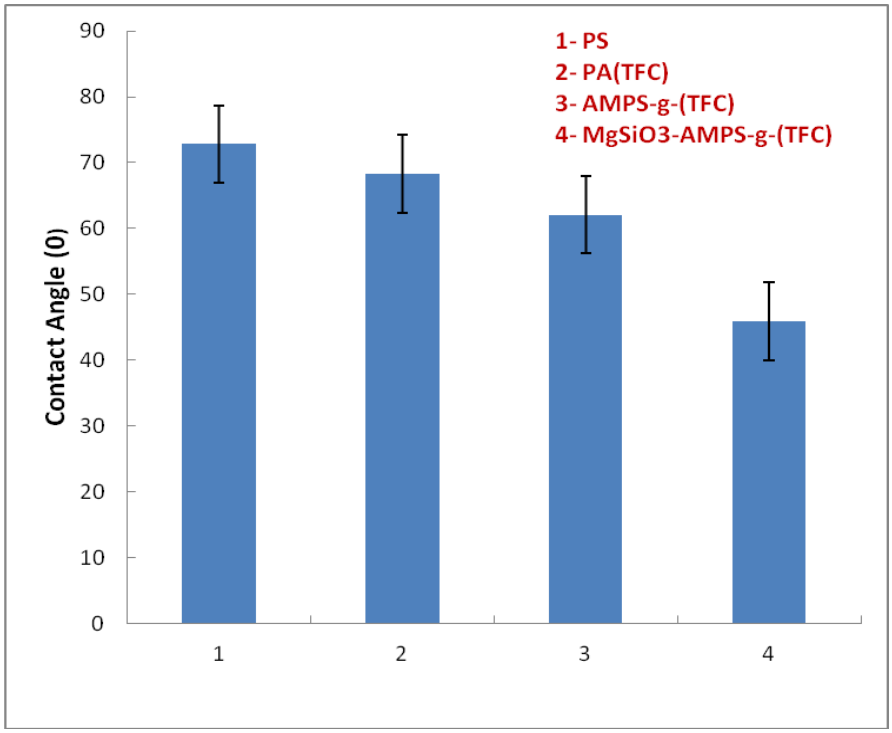

Figure 10.

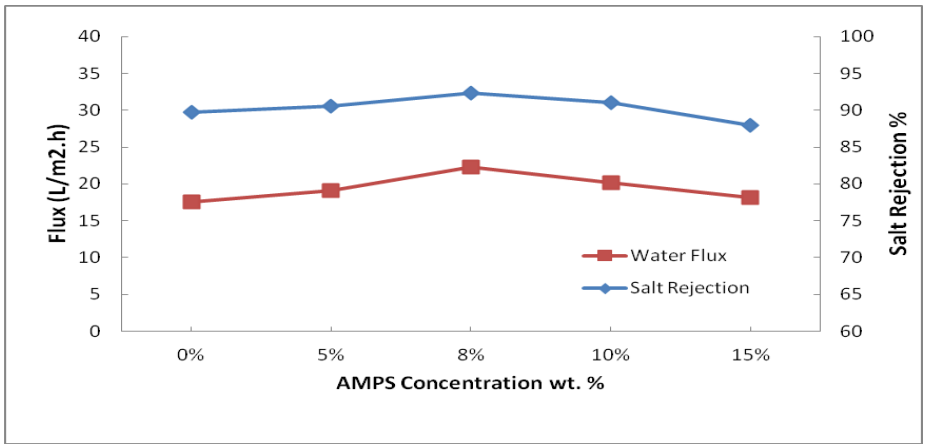

Figure 11.

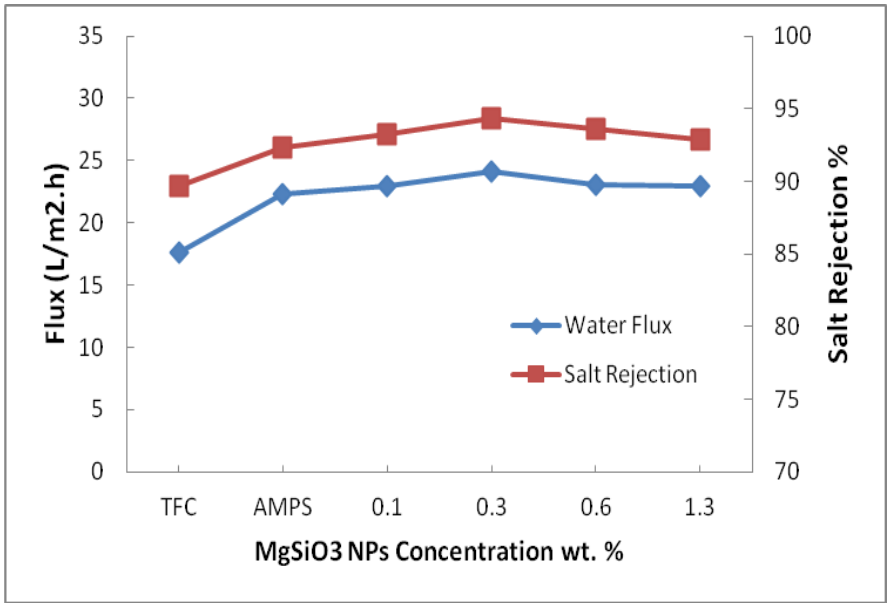

Figure 12.

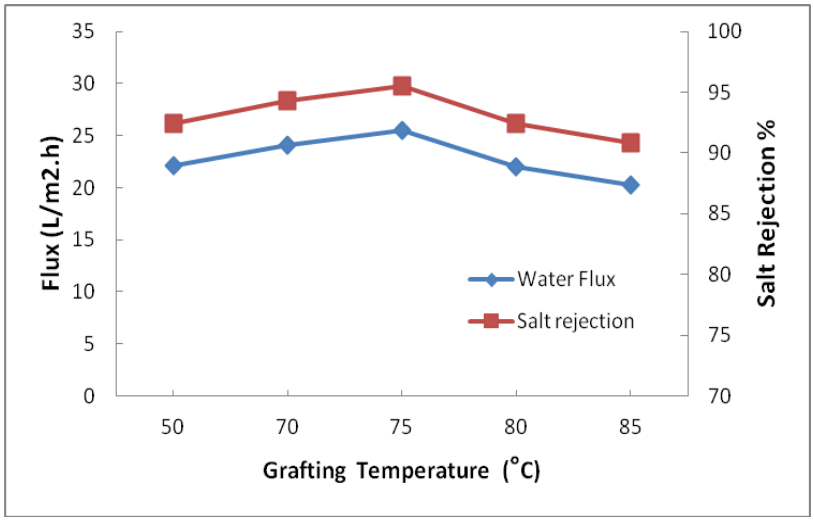

Figure 13.

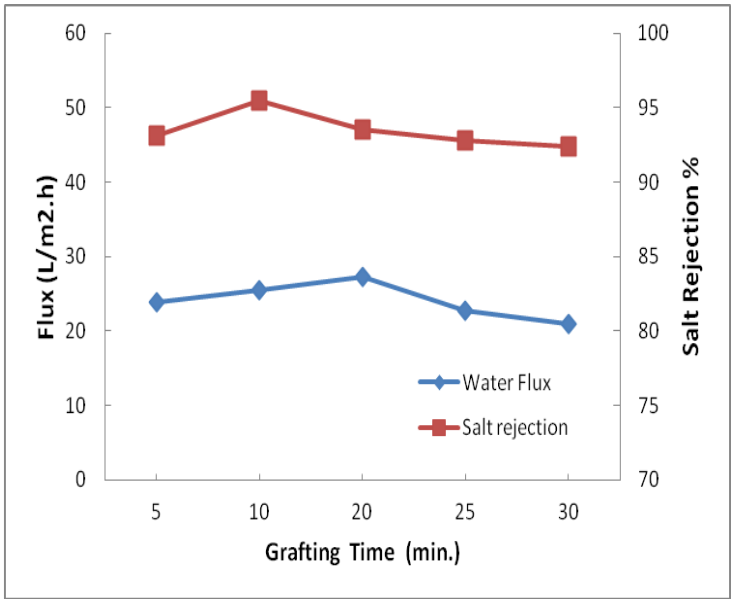

Scheme1.

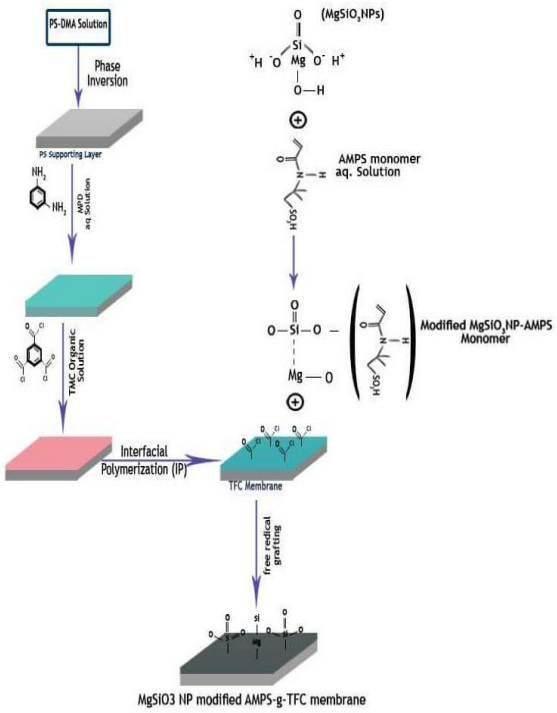

Scheme2.

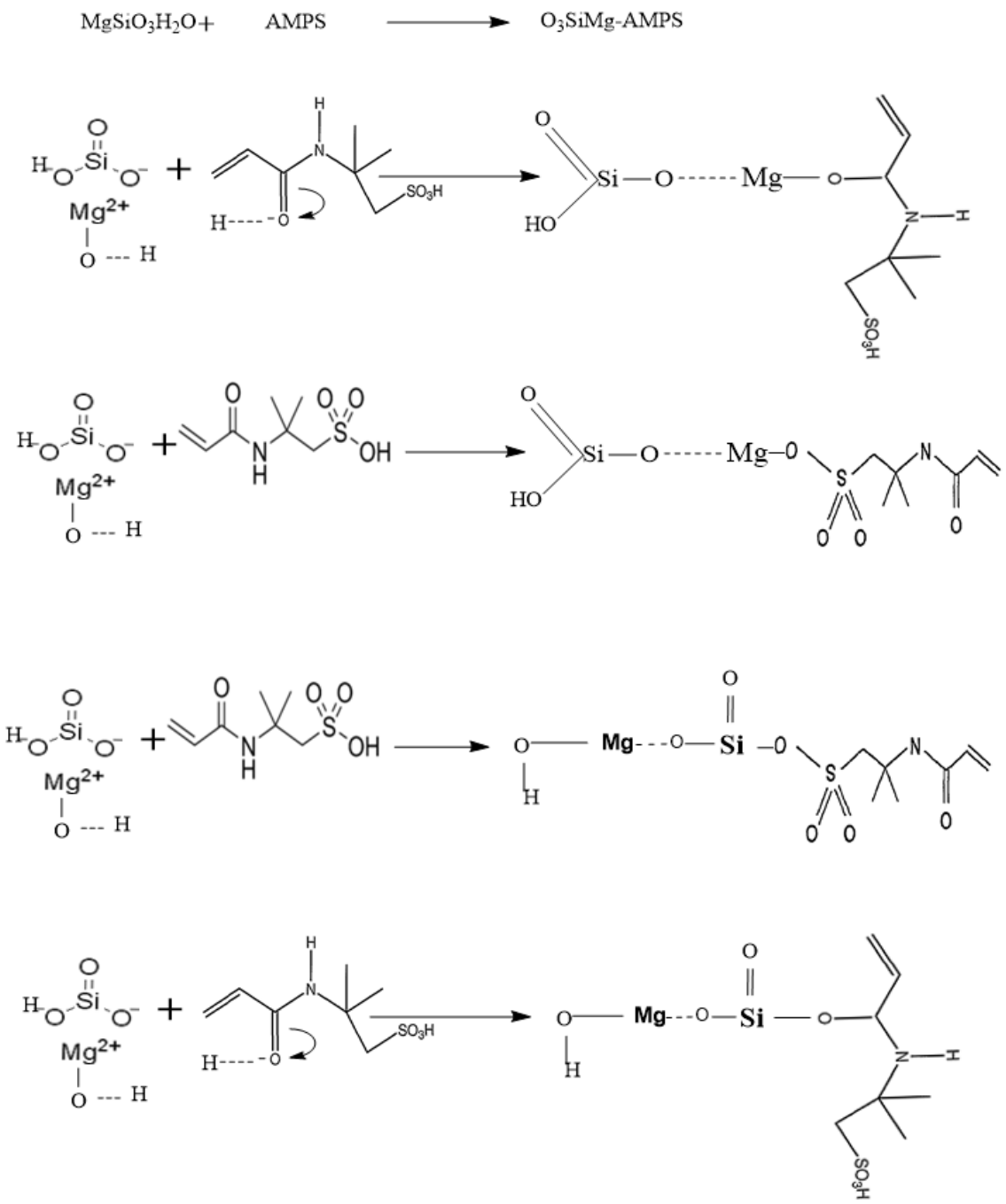

Table 1.

Membrane Type	**Pos. [2 θ]**	**d-spacing [A°]**	**Height [counts]**	**FWHM Left [2 θ.]**	**Rel. Int. [%]**
AMPS-g-TFC	26.2765	3.39170	10.72	0.2362	4.35
	38.1889	2.35670	246.38	0.1378	100.00
	44.4007	2.04034	183.76	0.0984	74.58
$MgSiO_3$ NPs modified AMPS-g-TFC	10.2852	8.60085	0.66	0.2362	0.16
	17.8318	4.97428	7.26	0.2362	1.72
	18.3740	4.82870	5.79	0.2362	1.38
	38.1082	2.36150	140.05	0.0787	33.28
	44.4324	2.03896	420.83	0.0984	100.00
	54.6609	1.67916	0.57	0.2362	0.14